This article has been accepted for inclusion in a future issue of this journal. Content is final as presented, with the exception of pagination.

Gastrointestinal Targeted Sampling and Sensing via Embedded Packaging of Integrated Capsule System

George E. Banis, *Student Member, IEEE*, Luke A. Beardslee, Justin M. Stine, *Member, IEEE*, Rajendra Mayavan Sathyam, and Reza Ghodssi, *Fellow, IEEE*

***Abstract*— Here, we introduce a wireless platform developed to leverage biochemical characteristics of various gastrointestinal (GI) secretions to selectively dissolve pH-sensitive polymers used as coatings over a 3-D printed biocompatible capsule, allowing fluid entry into sensing chambers containing capacitive sensors. Ingestible capsule technology is increasing prevalence in autonomously accessing regions of GI that otherwise require clinical intervention. Our platform is operated using a 3.3-V power source with sensors, possessing a 0.3–220-pF dynamic range with a sensitivity of 3.2×10^{-3} pF/mV that relay the change in capacitance to a smart system-in-package, which is then transmitted via Bluetooth low energy to an external Android phone. The system is tested with a variety of polymers, which are used in the pharmaceutical industry, to control dissolution at different GI regions characteristic of a specific pH profile. This real-time, cost-effective, and user-friendly platform will ultimately be used to test alternative coating materials that respond to specific biomarkers present in GI secretions, offering significant potential for enhancing gut diagnostics. [2018-0249]**

***Index Terms*— Ingestible systems, capsule, capacitive sensing, gastrointestinal tract, system integration.**

I. Introduction

CAPSULE-BASED integrated devices have recently been gaining traction as vehicles for sampling through the gastrointestinal (GI) tract for overcoming limitations in current medical techniques. To become a viable medical solution in its respective function, the autonomous diagnostic system must be able to navigate and function within the GI tract physiological environment, which is often chaotic and inhibitive to systems requiring high control [1]–[7]. With the wide range of potential applications, they are ubiquitous in academic settings, and few are making success in industry aiding practitioners in the clinical field [8]–[10]. One of the most successful commercially available examples is the capsule endoscope, such as the PillCam (Given Imaging ©), initially introduced as a solution to the limited achievable range during endoscopic procedures in the GI tract such as a colonoscopy or esophagogastroduodenoscopy [11]–[13]. The primary benefit of this technology over traditional endoscopy, other than that it does not require anesthesia or as much involvement from the clinician, is its enhanced ability to reach GI regions of difficult access. Overall, these detection technologies aim to understand the state of the GI environment in determining pathological conditions or obtaining previously inaccessible information.

Sampling GI fluids to obtain this information is used in diagnostics for isolating biomarkers related to specific GI pathologies, and targeting regions is critical for associating the biomarker with its source. Additional examples that have yet to mature to clinical implementation require specific sensing surface modifications with increasing target complexity, based on the biomarker of interest. One such device measures gas concentrations in the gut, which optical images cannot easily distinguish [2]. Though electrochemical gas sensors have been around since the 19th century, the novelty lies primarily with the integration of this sensor into an ingestible system, thereby offering potential for clinical evaluation that did not previously exist [14]. Another device uses fluorescence imaging to determine the occurrence of GI bleeding [6]. This device serves as another alternative to traditional endoscope procedures for real-time monitoring and is also more specific than using capsule endoscopy as discussed above. Additional examples warrant further discussions over the impact of the capsule-based biomedical devices, and a prevalent theme is the integration of low-power electronics and relevant sensors within a compact ingestible package [3]–[5], [7], [9], [15].

The basic components required for most real-time sensing with wireless signal transmission include: a sensor, microcontroller, signal transceiver, power supply, and a capsule-like package that can be swallowed [16]. However, for achieving more complex tasks, such as sensing, at the required size scale, energy becomes a significant limiting factor that demands controlled allocation of current to as few system modules as possible for minimal time durations. Furthermore, complex tracking systems are often required to monitor whether or not the sensor measurements are occurring in the appropriate region [17]–[20]. These systems can include cumbersome equipment that the patient must wear in the form of a

Manuscript received October 19, 2018; revised January 28, 2019; accepted January 30, 2019. This work was supported in part by the National Science Foundation through the ECCS Program under Award 1738211 and in part by the Maryland NanoCenter and its FabLab. Subject Editor H. Jiang. *(Corresponding author: George E. Banis.)*

G. E. Banis is with the Fischell Department of Bioengineering, University of Maryland, College Park, MD 20742 USA (e-mail: gbanis@umd.edu).

L. A. Beardslee is with the Institute for Systems Research, University of Maryland, College Park, MD 20742 USA (e-mail: labeardslee04@gmail.com).

J. M. Stine and R. M. Sathyam are with the Department of Electrical and Computer Engineering, University of Maryland, College Park, MD 20742 USA (e-mail: jmstine@terpmail.umd.edu; mayavan95@gmail.com).

R. Ghodssi is with the Institute for Systems Research, University of Maryland, College Park, MD 20742 USA, and also with the Department of Electrical and Computer Engineering, University of Maryland, College Park, MD 20742 USA (e-mail: ghodssi@umd.edu).

Digital Object Identifier 10.1109/JMEMS.2019.2897246

1057-7157 © 2019 IEEE. Personal use is permitted, but republication/redistribution requires IEEE permission.
See http://www.ieee.org/publications_standards/publications/rights/index.html for more information.

This article has been accepted for inclusion in a future issue of this journal. Content is final as presented, with the exception of pagination.

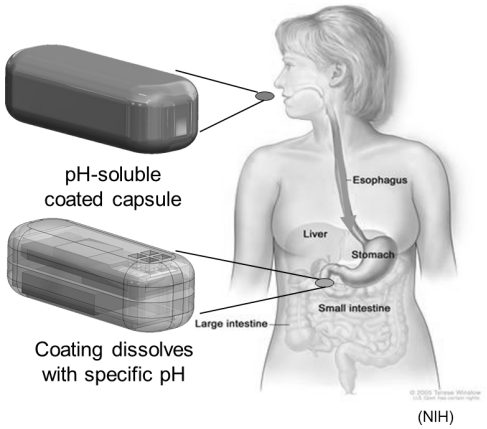

Fig. 1. Depiction of system outlook and application (Image credits: NIH). Polymer coatings are intended to dissolve at either the stomach (pH 1.5-3) or the duodenum (pH 7-8.5). At the duodenum, gastric acid-neutralizing bicarbonate is secreted from the pancreas via the sphincter of Oddi.

belt-like sensor array unit, and rely on magnetic or RF-based localization [21], [22].

In this work, a wireless capsule system is developed for monitoring the sampling potential at various targeted GI regions that (a) requires low power and (b) uses surrounding pH to approximate location. A 3-D-printed custom package encapsulates capacitive sensors, which are multiplexed and interfaced via a capacitive-voltage converter (CVC) with a Bluetooth system-in-package (SiP) that can pair with a mobile device via Bluetooth Low Energy (BLE). The capsule design possesses gratings that are plugged with different polymers, each for dissolving at various biochemical conditions to allow for selective fluid entry into a sensing chamber. Once the environmental condition is met, the grating-polymer opening is detected by the capacitive sensors, with fluid entry changing the dielectric property of the chamber.

A variety of coating strategies have been utilized previously for intestinal targeting. For example, some capsules implement time-controlled release coatings in the form of hydrophobic polymer layers (HPC), which are dependent on the weight and chemical composition as well as variations in GI transit [23]. However, these polymers are used to target specific regions, whereas the materials in this work are implemented with an interest in targeting the secretions. The polymers tested in this work, therefore, were chosen to demonstrate potential for sampling in a variety of regions in the GI tract based on pH, with an emphasis on sampling pancreatic secretions as depicted in Fig. 1. The transition in pH at the duodenum from acidic to neutral conditions due to reactions of gastric juices with pancreatic bicarbonate, which occurs over a time period of ∼30-60 minutes, offers a distinct event that is used in our design to target and sample pancreatic secretions. The gratings are filled with various formulations of pH-sensitive copolymers composed of acrylic and methacrylic acid that are currently used in the pharmaceutical industry for drug delivery to specific GI regions [24]–[26]. Different coating thicknesses are tested, as well as combinations of coatings for more complex sequences. Here, we discuss the design of the system packaging, electronics, and their miniaturization.

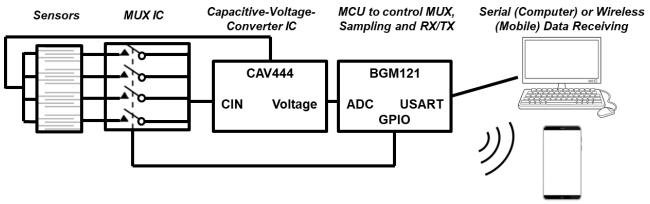

Fig. 2. System electronics overview. Circuit design includes a multiplexer (MUX) integrated circuit (IC), a capacitance-voltage-converter (CVC) IC, a 1.5 MHz step-up DC-DC converter, and a BLE system-in-package (SiP) micro-controller unit (MCU).

II. System Description

A. Sensors and System Electronics

Electrode patterns, consisting of four sensors dimensioned at 3 cm × 1 cm, were obtained through a standard "lift-off" process on 100 mm Pyrex wafers involving photolithography using NR9-1500PY photoresist, E-beam evaporation of Cr/Au (20 nm/200 nm) followed by the final "lift-off" step in acetone. Resulting interdigitated electrodes (IDEs), a total of 72 pairs, were 50 μm wide with 50 μm spacing and 2 mm length. IDE devices were then diced using a standard dicing saw (Microautomation).

The electronics, including various off-the-shelf integrated circuits (IC), used to operate the capsule are summarized in Fig. 2. In our configuration, four identical capacitive transducers are connected with a multiplexer as inputs (MUX IC, DG4052, Analog Microelectronics), each of which is measured using a CVC IC (CAV444, Analog Microelectronics). The voltage output is connected to the analog-to-digital converter (ADC), a part of a microcontroller unit (MCU, BGM121, Silicon Labs), which transmits the signal either serially to a computer via UART or wirelessly to a mobile device via BLE, respectively. General-purpose input/output (GPIO) pins from the MCU control the MUX to determine which sensor connects to the CVC. BLE is used as the wireless signal transmission technology because of the ease of interfacing with a smartphone, the availability of components that fit the needed form factor, and the availability of low-power components with a sleep mode. The rechargeable 14 mAh at 3.3 V lithium polymer battery (Powerstream) was the optimal choice for the design satisfying the constraint of small form factor and source enough power for the wireless transmission. Fig. 3 presents the calibration of the ADC output potential, using standard capacitors. The resulting capacitance recorded when the sensors are exposed to air and phosphate buffer were 39.15 ± 1.25 and 95.93 ± 1.92 pF, respectively (n = 4).

B. Capsule Package Design and Materials

Each capsule is designed in SolidWorks (Dassault Systemes) and 3-D printed from a biocompatible acrylic resin (MED610) from an Objet30 Pro (Stratasys) to assess the feasibility and utility of the capsule packaging and achieve the desired form factor according to previously determined standards for capsule endoscopy [11], [12]. The capsule designs and prints in Fig. 4 are used for experiments using the external circuit layout. Gratings consisting of 0.4 mm × 0.4 mm hole arrays

This article has been accepted for inclusion in a future issue of this journal. Content is final as presented, with the exception of pagination.

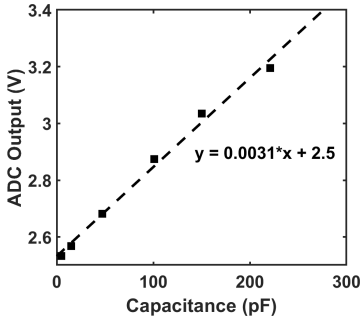

Fig. 3. (a) Circuit calibration with standard capacitors across four multiplexed inputs. The resulting system senses capacitive changes in the 0.8-220 pF dynamic range with a sensitivity of 3.2 × 10-3 pF/mV and operated using a 3.3 V source.

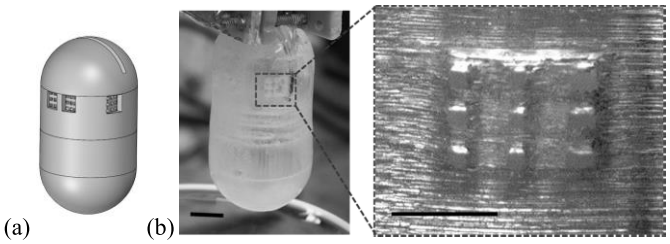

Fig. 4. (a) CAD model of the capsule used with external circuit. (b) 3-D-printed version with zoomed up view of gratings. Scale bar = 1 mm.

were positioned over sensor regions for fluid accessibility into the hollow space. A slot with 600 μm thickness and 1.1 cm width was created to allow for sensor insertion while sensor contact pads remained on the outside of the capsule. The sensor and slot interface was epoxied for sealing, then the capsule was immersed, for 1-2 seconds, in a highly viscous 14% Eudragit S 100 (Evonik), a methacrylic acid–methyl methacrylate copolymer with 0.3% sodium laurylsulfate, in methanol for dip-coating individual layers over up to 5 successive cycles. No bubbles appeared, indicating the polymer solution was not displacing air in the capsule space and therefore did not cause the capsule to fill and contact the sensors. Cross-sectioned images were taken of the grating regions, two of which (0 and 1 coating) are depicted in Fig. 5a and b, and analyzed for uniformity over grating and non-grating regions in Fig. 5c. Dip-coating was used in this work due to its reliability for producing highly uniform surfaces and compatibility with our capsule system. The compatibility stems from the geometry of the capsule compared to tablets and pellets, as well as the presence of an internal electronics system, for which more conventional coating methods that use vibration or higher temperatures are more compatible. There is potential for improving uniformity in the process through more precision in the velocity of insertion and removal of the capsule from the dip-coating solution. Electrostatic dry powder application via spray-nozzle can also be considered as an alternative method in future iterations [27].

C. System Miniaturization and Assembly

The circuit was embedded onto a four-layer printed circuit board (PCB, 25 mm × 10 mm × 2 mm) made of FR4 with a silver finish (Sunstone). The PCB is depicted in Fig. 6a, indicating the pins used to connect to the battery, the contact pads

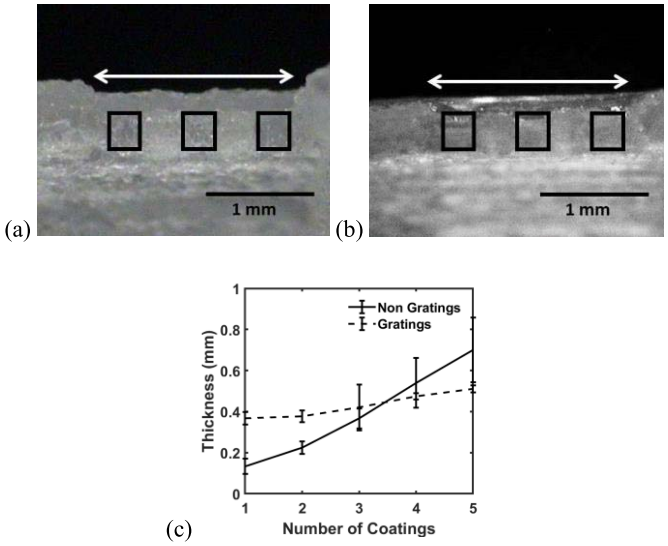

Fig. 5. Cross-sectional optical images of the sampling gratings (a) uncoated and (b) with 1 coating of polymer, where white arrows indicate the grating locations and black boxes indicate the inlets. (c) Characterization of polymer coating thickness vs. number of dipping steps from both non-grating and grating regions over the 3-D-printed capsule surface (n = 3). Scale bar = 1 mm.

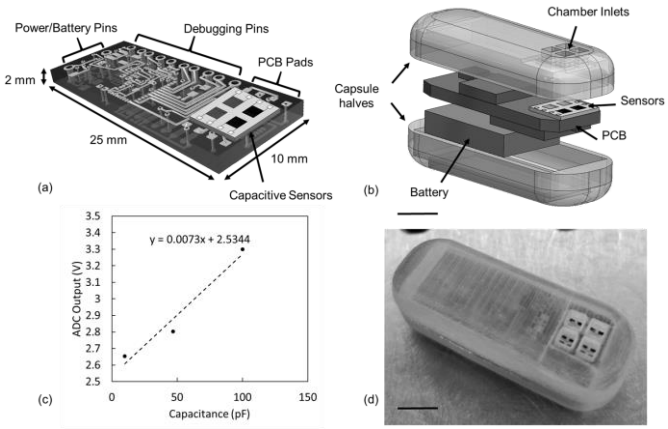

Fig. 6. (a) PCB rendering with sensor die fixated between designated pads using epoxy. Contact was made by curing conductive silver ink. (b) Schematic of the assembled capsule setup. (c) Calibration of BLE MCU at the PCB level using standard capacitors. Sensitivity increased from 3.6 to 7.3 pF/mV from the breadboard to PCB level, respectively. (d) Photograph of assembled capsule. Scale bar = 5 mm unless otherwise specified.

for connecting to the sensors, and the pins for programming the MCU. The schematic of the assembled capsule setup is depicted in Fig. 6b. New sensors, with a smaller footprint to fit between the PCB contact pads and required capacitance range, depicted in Fig. 6c, were fabricated as described previously. The new sensor dimensions possessed 10 μm wide with 10 μm spacing and 1.5 mm length. Most experiments were performed with the PCB connected to a power supply through wires instead of the battery, as the battery performance was optimized at this point for only 1 hour whereas certain experiments required longer durations. The PCB and wires were encapsulated in conformal coating, consisting of acrylic copolymer (CAIG Laboratories), and inserted into a modified

This article has been accepted for inclusion in a future issue of this journal. Content is final as presented, with the exception of pagination.

3-D printed capsule for directly interfacing the gratings with the sensors. A photograph of the assembled capsule is depicted in Fig. 6d.

D. Experimental Procedures for pH Sequences

For the circuit layout external to the capsule, the sensor contact pads were connected to the circuit with a custom insert with spring-loaded pins. The capacitance was then transmitted serially from the BGM121 wireless starter kit (WSTK) via UART. All capsules were inserted into heated solutions (37°C) under stirring conditions (250 RPM). A measurement sequence was defined to determine polymer degradation at various pH states, according to a known pH dissolution profile. Beginning with measurements in air for 5 min, the capsule was then inserted into a solution with a negative control pH, the level of which depended on the polymer plug used. The pH was then adjusted progressively to the positive control pH that was expected to cause dissolution. Solutions beginning with acidic pH consisted of 0.1 M acetic acid (pH 2.9), while solutions beginning with neutral pH were 0.1 M phosphate buffer (pH 7.6). These pH levels were chosen to reflect the pH range of target regions of the GI tract, specifically the stomach and small intestine for acidic and neutral secretions, respectively [28], [29]. Progressive pH adjustments were performed every 30 min for acid- and neutral-solutions via droplets of 1 M phosphoric acid and 1 M sodium hydroxide, respectively, measured using a standard pH meter (Oyster-10, Extech Industries). The coating procedure discussed in Section IIb was repeated, three coatings each, for Eudragit formulations L 100 and E PO, intended to dissolve at >pH 6 and <pH 5 ranges, respectively (Evonik). The pH progression for their respective experiments were 2.9 to 7.6 and 7.6 to 2.9 in discrete increments of ∼1.0 to control for the sensor responses in non-soluble pH conditions. The procedure was repeated with an initial 3 coatings of L 100, followed by 3 coatings of E PO formulations (depicted in the coating rendering in Fig. 8d), and tested with a pH sequence of 7.6 to 2.9 to 7.6. Once the positive control pH was reached, the capsule was removed from solution for 10 min and signal transmission was terminated.

The miniaturized system of the capsule with inserted PCB was coated with three coatings of E PO solution, then immersed into both pH 7.6 and pH 2.9 solutions while recording capacitance over time. The recorded capacitance was obtained via BLE by pairing with an Android phone, initiated via a modified application from the manufacturer. The data was stored onto the mobile device as a text file and analyzed in a desktop PC. Photographs were taken at the 0, 30 minute, and 1 hour time points during immersion to periodically observe progress in coating dissolution. All polymer solutions were 30%w/v in methanol and dyed for enhanced visualization.

All data was plotted using a custom MATLAB (MathWorks) graphical user interface (GUI). For the WSTK obtained data, the signals were recorded into a text file using RealTerm (Company?). For the PCB layout, the recorded capacitance was obtained via BLE by pairing with an Android phone, initiated via a modified application from the manufacturer (SiliconLabs). The data was stored onto the mobile device as a text file, sent to a computer, and analyzed with the MATLAB GUI.

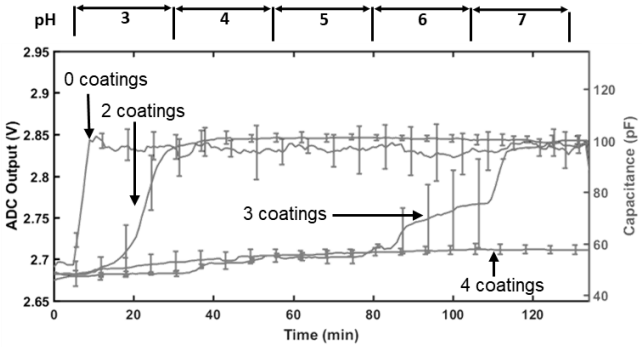

Fig. 7. Sensor responses (inserted into buffer at 5 min) of capsules with different numbers of S 100 coatings (0, 2, 3, and 4, respectively) with increasing pH using titers of 1 M NaOH (n = 4). Chamber filling is characterized by a capacitance change of ∼50 pF from the initial capacitance in air. For each formulation, it was determined that 3 coatings was optimal for the w/v% used.

III. Experimental Results

A. Sensor Responses

The sensor responses, both in voltage at the ADC and corresponding capacitance, for capsules dipped in increasing coatings are depicted in Fig. 7. For 0 coatings, the point at which the capsule was inserted into buffer is indicated by the sharp increase in capacitance at around 5 minutes due to immediate entry of buffer, causing an instant change in the medium dielectric constant. The data for 1 coating was omitted due to the lack of sealing of the gratings, producing a similar result as that of the 0 coating sequence. With the increase in number of coating layers, the rate of the capacitance change is reduced significantly, recorded at approximately 16.0, 5.6, and 1.1 pF/min for 0, 2, and 3 coatings, respectively. The system with 4 coatings did not open within the 140 minute duration, though experiences some drift in capacitance due to a potential presence in moisture or other source. As expected, additional dip coatings corresponded to an increase in the fluid entry time, allowing us to tailor the packaging to different time scales based on coating thickness from corresponding measurements in Fig. 5c.

B. Coating Variety and Combinations

After varying the coating thickness, we tested polymer formulations that would dissolve at different pH ranges. Real-time capacitance measurements for the pH sequences of the L 100 and E PO coatings are depicted in Fig. 8a-b, respectively, with the latter pH in which the coatings were intended to dissolve enough to achieve sampling. The resulting capacitance indicated that sampling occurred in representative ranges (neutral for L 100 and acidic for E PO), implying both the compatibility for different material usage as coatings and their potential as the system package to target different GI regions. To allow for sampling in a more complex

This article has been accepted for inclusion in a future issue of this journal. Content is final as presented, with the exception of pagination.

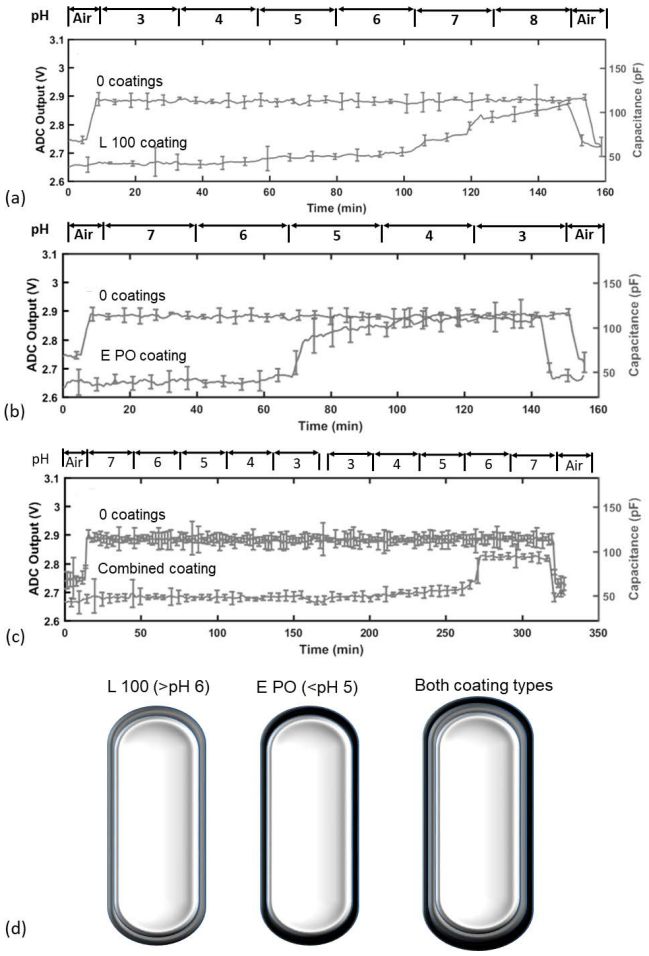

Fig. 8. Sensor responses inserted into capsules with different types of coatings (3 dip-coatings each) compared to uncoated controls: (a) L 100, (b) E PO, and (c) combined coatings, where E PO is outer-most and L 100 is be-tween the 3-D-printed capsule and the E PO layers (n = 4). (d) Capsule rendering for displaying coating conditions for each sequence.

sequence such as that expected between the mouth and the small intestine (neutral – acidic – neutral pH, respectively), we layered 3 coatings each of L 100 and E PO sequentially over the capsule surface, depicted in Fig. 8c. The resulting measurements with the sequence used, consisting of pH 7 to 3 to 7, are displayed in Fig. 8c, where the increase in capacitance to saturation point occurs at the return to neutral pH. This indicates that the E PO coating was able to protect the L 100 coating early on while transitioning to pH 3, while the L 100 coating ensured the gratings were sealed until the system returned to neutral pH. While it appears the saturation capacitance of the combined coating does not reach that of the uncoated control, it is possible that this difference could have occurred as a result of reduced contact between the sensor surface and buffer, potentially through the presence of polymer residue or a bubble on the surface; increasing surface hydrophilicity of the electrodes may improve this complication in future works.

It is important to note that the slope between baseline capacitance to the saturated capacitance varied with polymer type. This difference in timing was most likely affected by

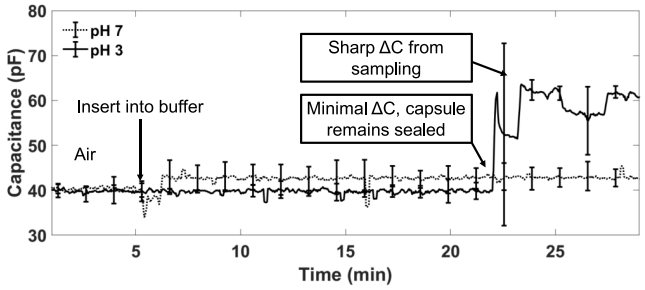

Fig. 9. Real-time representative trials of capacitance measurements obtained via BLE of 3x coated capsule immersed in control (neutral, pH 7) (dotted) and specific target (solid) pH (acidic, pH 3). The rapid increase in capacitance represents buffer inflow and contact with capacitor sensors, representing targeting of coating dissolution. (N = 2).

variations in each polymer's dissolution rate. Alternatively, it is possible that it was also affected by their respective apparent viscosity at the solution concentration used (L 100: 60-120 mPa-s, S 100: 50-200 mPa-s, E PO: 3-6 mPa-s, according to the manufacturer), which varies the amount of plug infill during the initial coating and polymer remaining in subsequent steps, which would also impact the rate of solvent dissipation, specifically the methanol to air, with each coating. No observable differences in coating appearance were seen during the coating process with each interval.

C. Assembled Capsule Coating and Sensor Responses

Assembled capsules were tested to ensure functionality in the fully integrated system compared to the breadboard-level circuit. The insulated PCB with the sensor connected were inserted alone into neutral buffer, before insertion into the capsule, resulting in a spike and saturation in capacitance similar to the previous immersion experiments (Data not shown). The capacitance measurements produced from the polymer coated capsule in both neutral and acidic buffer are depicted in Fig. 9. Here, we observed that the sensors continued to measure the same capacitance from beginning to end for the neutral buffer, indicating there was a lack of buffer inflow and therefore the plug remained intact. For the coated capsule, however, we observe an increase in capacitance after about 18-22 minutes post insertion into acidic solution. Interestingly, we observed that the change in capacitance is only ∼20 pF compared to the 50 pF shift for the external electronics, which we found was due to the presence of additional parasitic capacitances introduced during the assembly process. However, the relative change in capacitance remains comparable, as well as the distinct increase the acidic pH compared to within the neutral pH upon dissolution of the polymer coating.

For additional qualitative validation, the photographs in Fig. 10 depict little to no change in the capsule coating throughout the neutral buffer sequence, whereas the coating is mostly dissolved – both in the gratings the non-grating regions of the capsule surface – as the experiment with the acidic buffer progressed. This result is consistent with the recorded capacitance measurements, indicating a specific time point at which the buffer contacted the sensor. Based on the previous experiments, we could tailor this fluid intake for different

This article has been accepted for inclusion in a future issue of this journal. Content is final as presented, with the exception of pagination.

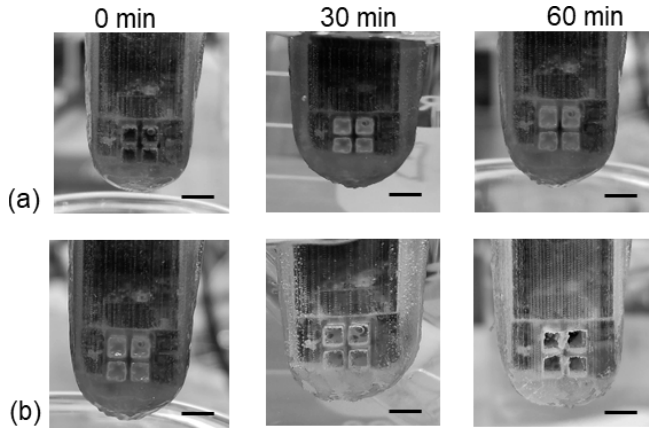

Fig. 10. Progression of polymer coating throughout (a) control and (b) pH-based dissolution tests. Beginning, 30 minutes, and 1 hour immersion periods are from the left, middle, and right, respectively. Scale bar = 3 mm.

timing windows by varying coating thicknesses, as well as coating materials.

IV. Conclusion

In this work, we present a wireless microsystem capable of targeted fluid sampling based on pH-selective dissolution of polymer coatings. Due to the interface with the phone app and usage of off-the-shelf components for the circuit, this system enables a user-friendly and cost-effective means to monitor real-time data acquisition of GI fluid sampling dependent on targeted physiological characteristics.

Various limitations were noted during optimization and analysis. Future capsule structures will likely be tailored by using fluid flow mechanical simulations to design enhanced inlet geometries that would enable more rapid sampling upon coating dissolution. The plug infill process could be improved to become more precise, accounting for viscosity of polymer solution for uniformity across multiple coatings while continuing to maintain an effective seal. Furthermore, the slopes used to determine rate of sampling may be affected by the presence of potential air bubbles in the sensing chamber, delaying the ability of the buffer solution to contact the sensor surface and thus reducing the accuracy of our assumed sampling rate. Ultimately, we acknowledge that this work is performed on the benchtop, thereby neglecting the impact of variations in GI transit time or the naturally-occurring mechanical stimuli from peristalsis and general motion.

Our future work consists of using additional coating and plug materials to those that would react with more specific analytes present in GI fluids, such as peptide- or polysaccharide-based coatings for dissolving with environmental digestive enzymes from pancreatic secretions. This platform will be adapted for multiple sampling and sensing chambers, individually coated with a variety of biomarker-specific materials toward isolated biomolecular identification and therefore enhanced utility and customization to diagnose different GI pathologies.

References

[1] G. E. Banis, L. A. Beardslee, J. M. Stine, and R. Ghodssi, "Enteric & 3D-printed hybrid package for sampling in digestive regions," in *Proc. Solid-State Sens., Actuators Microsyst. Workshop*, 2018, pp. 96–97.

[2] K. Kalantar-Zadeh *et al.*, "Intestinal gas capsules: A proof-of-concept demonstration," *Gastroenterology*, vol. 150, no. 1, pp. 37–39, 2015.

[3] J. L. Gonzalez-Guillaumin, D. C. Sadowski, K. V. I. S. Kaler, and M. P. Mintchev, "Ingestible capsule for impedance and pH monitoring in the esophagus," *IEEE Trans. Biomed. Eng.*, vol. 54, no. 12, pp. 2231–2236, Dec. 2007.

[4] P. Demosthenous and J. Georgiou, "An ingestible, NIR-fluorometric, cancer-screening capsule," in *Proc. 37th Annu. Int. Conf. IEEE Eng. Med. Biol. Soc. (EMBC)*, Aug. 2015, pp. 2143–2146.

[5] C. M. Caffrey, K. Twomey, and V. Ogurtsov, "Development of a wireless swallowable capsule with potentiostatic electrochemical sensor for gastrointestinal track investigation," *Sens. Actuators B, Chem.*, vol. 218, pp. 8–15, Oct. 2015.

[6] A. Nemiroski, M. Ryou, C. C. Thompson, and R. M. Westervelt, "Swallowable fluorometric capsule for wireless triage of gastrointestinal bleeding," *Lab Chip*, vol. 15, no. 23, pp. 4479–4487, Dec. 2015.

[7] W. Yu, R. Rahimi, M. Ochoa, R. Pinal, and B. Ziaie, "A smart capsule with GI-tract-location-specific payload release," *IEEE Trans. Biomed. Eng.*, vol. 62, no. 9, pp. 2289–2295, Sep. 2015.

[8] S. S. Mapara and V. B. Patravale, "Medical capsule robots: A renaissance for diagnostics, drug delivery and surgical treatment," *J. Control. Release*, vol. 261, pp. 337–351, Sep. 2017.

[9] C. M. Caffrey, O. Chevalerias, C. O'Mathuna, and K. Twomey, "Swallowable-capsule technology," *IEEE Pervasive Comput.*, vol. 7, no. 1, pp. 23–29, Jan./Mar. 2008.

[10] K. Kalantar-Zadeh, N. Ha, J. Z. Ou, and K. J. Berean, "Ingestible sensors," *ACS Sensors*, vol. 2, no. 4, pp. 468–483, 2017.

[11] D. Friedel, R. Modayil, and S. Stavropoulos, "Colon capsule endoscopy: Review and perspectives," *Gastroenterol. Res. Pract.*, vol. 2016, Aug. 2016, Art. no. 9643162.

[12] S. N. Adler and Y. C. Metzger, "PillCam COLON capsule endoscopy: Recent advances and new insights," *Therapeutic Adv. Gastroenterol.*, vol. 4, no. 4, pp. 265–268, 2011.

[13] M. Rasouli *et al.*, "Therapeutic capsule endoscopy: Opportunities and challenges," *J. Healthcare Eng.*, vol. 2, no. 4, pp. 459–471, 2011.

[14] N. Opitz and D. W. Luebbers, "Theory and development of fluorescence-based optochemical oxygen sensors: Oxygen optodes," *Int. Anesthesiol. Clin.*, vol. 25, no. 3, pp. 177–197, 1987.

[15] S. Yim, E. Gultepe, D. H. Gracias, and M. Sitti, "Biopsy using a magnetic capsule endoscope carrying, releasing, and retrieving untethered microgrippers," *IEEE Trans. Biomed. Eng.*, vol. 61, no. 2, pp. 513–521, Sep. 2013.

[16] C. Van de Bruaene, D. De Looze, and P. Hindryckx, "Small bowel capsule endoscopy: Where are we after almost 15 years of use?" *World J. Gastrointestinal Endoscopy*, vol. 7, no. 1, pp. 13–36, Jan. 2015.

[17] J. Worsøe *et al.*, "Gastric transit and small intestinal transit time and motility assessed by a magnet tracking system," *Gastroenterology*, vol. 11, no. 1, p. 145, 2011.

[18] N. Mehmood and S. M. Aziz, "Magnetic sensing technology for *in vivo* tracking," in *Proc. Int. Conf. Emerg. Technol.*, Oct. 2012, pp. 1–4.

[19] I. Umay, B. Fidan, and B. Barshan, "Localization and tracking of implantable biomedical sensors," *Sensors*, vol. 17, no. 3, p. 583, 2017.

[20] E. A. Johannessen, L. Wang, S. W. Reid, D. R. Cumming, and J. M. Cooper, "Implementation of radiotelemetry in a lab-in-a-pill format," *Lab Chip*, vol. 6, no. 1, pp. 39–45, Dec. 2006.

[21] M. Yu, "M2A capsule endoscopy. A breakthrough diagnostic tool for small intestine imaging," *Gastroenterol. Nurses Associates*, vol. 25, no. 1, pp. 24–27, 2002.

[22] Y. Ye, "Bounds on RF cooperative localization for video capsule endoscopy," Ph.D. dissertation, Worcester Polytech. Inst., Worcester, MA, USA, 2013.

[23] A. K. Philip and B. Philip, "Colon targeted drug delivery systems: A review on primary and novel approaches," *Oman Med. J.*, vol. 25, no. 2, pp. 79–87, Apr. 2010.

[24] M. Puccetti, S. Giovagnoli, T. Zelante, L. Romani, and M. Ricci, "Development of novel indole-3-aldehyde-loaded gastro-resistant spray-dried microparticles for postbiotic small intestine local delivery," *J. Pharmaceutics Sci.*, vol. 107, no. 9, pp. 2341–2353, 2018.

[25] E. T. Cole *et al.*, "Enteric coated HPMC capsules designed to achieve intestinal targeting," *Int. J. Pharmaceutics*, vol. 231, no. 1, pp. 83–95, 2002.

[26] K. Whitehead, Z. Shen, and S. Mitragotri, "Oral delivery of macromolecules using intestinal patches: Applications for insulin delivery," *J. Control. Release*, vol. 98, no. 1, pp. 37–45, 2004.

This article has been accepted for inclusion in a future issue of this journal. Content is final as presented, with the exception of pagination.

[27] Y. Yang, L. Shen, F. Yuan, H. Fu, and W. Shan, "Preparation of sustained release capsules by electrostatic dry powder coating, using traditional dip coating as reference," *Int. J. Pharmaceutics*, vol. 543, nos. 1–2, pp. 345–351, May 2018.
[28] L. P. Degen and S. F. Phillips, "Variability of gastrointestinal transit in healthy women and men," *Gut*, vol. 39, no. 2, pp. 299–305, Aug. 1996.
[29] L. R. Johnson, *Physiology of the Gastrointestinal Tract*. New York, NY, USA: Academic, 2012.

George E. Banis (S'18) was born in Hillsborough, NJ, USA, in 1991. He received the B.S. degree in biomedical engineering with a concentration in electrical engineering from The College of New Jersey (TCNJ), Ewing, NJ, USA, in 2014. He is currently pursuing the Ph.D. degree in bioengineering with the MEMS Sensors and Actuators Laboratory, University of Maryland, College Park, MD, USA.

From 2011 to 2013, he was an MUSE Research Fellow with TCNJ, focused on computational modeling of cardiorespiratory function. He is currently a fellow of the Future Faculty Program with the University of Maryland. His current research interests include the design of ingestible integrated systems for gastrointestinal sampling and analysis, specifically toward management of pancreatic pathologies, with an emphasis on applied materials, biosensors, and micro-/nanofabrication technologies for applied diagnostics in healthcare.

Mr. Banis received several travel and presentation awards from TRF, AVS, BMES, and at the Global Grand Challenges Summit in 2017, among others.

Luke A. Beardslee was born in Boston, MA, USA, in 1984. He received the B.S. and M.Eng. degrees in electrical and computer engineering from Cornell University in 2007, the Ph.D. degree in electrical engineering from the Georgia Institute of Technology in 2011, and the Medical degree from the Albany Medical College in 2015.

He has also completed a General Surgery Internship. He has held several research positions including as a research scientist with the Research Foundation for the State of New York, SUNY IT Center for Nanoscale Science and Engineering, Albany, NY, USA, and as a visiting scientist with the University of Maryland, College Park. His research interests include micro/nanoscale fabrication, MEMS sensors, and embedded systems for implantable, ingestible, and environmental applications.

Justin M. Stine (M'15) was born in Clinton, MD, USA, in 1992. He received the B.A. degree in physics and mathematics from the St. Mary's College of Maryland, St. Mary's City, MD, USA, in 2014. He is currently pursuing the M.S. degree in electrical engineering with the University of Maryland, College Park, MD, USA.

From 2015 to 2017, he was a Teaching Assistant with the Department of Electrical and Computer Engineering (ECE), University of Maryland. His research interests include the development of embedded systems, specifically design and integration of readout circuits with fabricated micro/nanoscale sensors toward environmental monitoring. He was a recipient of the ECE Distinguished TA Award in 2017.

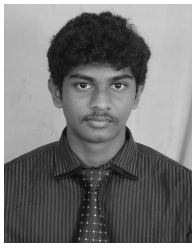

Rajendra Mayavan Sathyam was born in Virudhunagar, India, in 1995. He received the B.E. degree in electrical and electronics engineering from Anna University, Chennai, in 2017. He is currently pursuing the M.Eng. degree in robotics with the University of Maryland.

He was involved in developing the electronics for an automated hydroponics system with the St. Joseph's College of Engineering. In 2018, he joined MSAL, where he focuses on developing the software and hardware for MEMS devices, aimed toward sampling real time data from the GI tract using ingestible technology and enabling minimally invasive diagnostics and treatment of diseases.

Reza Ghodssi (F'15) was the Director of the Institute for Systems Research (ISR) from 2009 to 2017. During this time, he launched a number of interdisciplinary initiatives such as the Maryland Robotics Center and the Brain and Behavior Initiative, aimed at enhancing the impact of ISR research efforts on society while building a more interactive faculty, staff, and student community across different disciplines in the institute. He is the Herbert Rabin Distinguished Chair of engineering and the Director of the MEMS Sensors and Actuators Lab, Department of Electrical and Computer Engineering, and ISR, University of Maryland. He is a Distinguished Scholar–Teacher with the University of Maryland. He has authored or co-authored over 148 journal publications and 323 refereed conference papers. He is the Co-Editor of the *MEMS Materials and Processes* Handbook published in 2011. He holds eight U.S. patents, with another seven pending. His research interests are in the design and development of micro/nano/bio devices and systems for chemical and biological sensing, small-scale energy conversion, and harvesting with a strong emphasis toward healthcare applications.

Mr. Ghodssi is a fellow of IEEE, AVS, and ASME. He is an Associate Editor of the *Journal of Microelectromechanical Systems* and *Biomedical Microdevices*.